A Protection Method for Inverter-based Microgrid Using Current-only Polarity Comparison

Bin Wang and Liuming Jing

***Abstract*—The design of an effective protection system for inverter-based microgrids is a complicated engineering challenge. This is due to the fact that inverters have limited fault current capabilities, and that the conventional overcurrent protection is not suitable for inverter-based microgrids. This paper introduces a novel protection method for inverter-based microgrid using a current-only polarity comparison. The proposed method is based on the phase difference between the pre-fault and fault current components. The method responds to faults in both grid-connected and autonomous operation modes and provides a new way to identify faulted sections. Simulations of an inverter-based microgrid with a relay model are conducted using PSCAD/EMTDC software. The results show that the proposed method can detect faults in inverter-based microgrids.**

***Index Terms*—Distributed energy resources, inverter, microgrid protection, fault current.**

I. Introduction

In recent years, there have been significant changes in power systems, as centralized generation facilities have been replaced by smaller, more distributed energy resources (DERs). In particular, an increasing number of DERs have been integrated into distribution systems. Most DERs employ renewable energy resources such as photovoltaic (PV) generation, wind turbine generation and combined heat and power. The utilization of DERs confers many advantages such as reducing transmission losses, improving power quality, and interfacing with clean energy (e.g., wind and solar). Furthermore, a cluster of loads and DERs operates safely and efficiently within a local distribution network but can also be operated in the islanded mode in a small area of distribution networks, a configuration known as a microgrid [1]-[3]. Inverter-based microgrids usually contain voltage source inverter (VSI) interfaced DERs. And inverter-based microgrids have characteristics such as low inertia and small fault currents. However, the protection of inverter-based microgrids poses a technical challenge [4]-[8].

The protection system for inverter-based microgrids must ensure the safe operation in both grid-connected and autonomous modes, and respond to both grid and microgrid faults [9]-[12]. The large difference in fault current between grid-connected and autonomous modes presents challenges to microgrid protection. In the grid-connected operation mode, microgrid fault currents are large because the utility grid contributes to the fault current. Conventional overcurrent protection can be activated in this scenario. However, in autonomous mode, the fault current is very small. The output current of the inverter-based DERs is usually limited to 1.2 p.u. of their rated current, determined by the short-time current-carrying capacity of the semiconductor switches. The conventional overcurrent relay will be invalid in this case [13]-[16]. When a fault occurs in the microgrid, the faulted section should be identified and isolated so other parts of the microgrid can supply electric power normally. A microgrid is designated as a secondary distribution system and is supplied by a step-down transformer. Microgrids can fall into different grounding categories such as un-grounded, uni-grounded and multi-grounded types [17]. The grounding issues should also be considered in the microgrid protection system.

The protection methods for inverter-dominated microgrids can be classified into directional overcurrent relay based method, distance relay based method, current differential based method, voltage based method, traveling wave based method and fault current source based method. Reference [18] proposes a protection scheme equipped with directional overcurrent relays. However, the mechanism for activating the overcurrent relay with a small fault current is not described. The distance protection proposed in [19] has been previously evaluated in a radial distribution feeder. However, the sensitivity of the relay decreases due to the effect of the DER.

Reference [20] proposes a communication-based differential sequence component protection scheme for isolated microgrids. A data mining approach is used to identify the relay settings and parameters. However, the method requires a

Manuscript received: October 29, 2018; accepted: July 8, 2019. Date of Cross-Check: July 8, 2019. Date of online publication: November 26, 2019.

This work was supported by the China National Key Research and Development Program (No. 2017YFB0902802), the Science and Technology Project of State Grid Corporation of China (No. 52094017003D), and the China Postdoctoral Science Foundation (No. 2017M620777).

B. Wang and L. Jing (corresponding author) are with the State Key Laboratory of Power System, Department of Electrical Engineering, Tsinghua University, Beijing 100084, China (e-mail: binw_ee@mail.tsinghua.edu.cn; liuming_mark@126.com).

DOI: 10.35833/MPCE.2018.000722

high-bandwidth communication channel.

During the fault period in a microgrid, the protection based on *abc-dq* transformation of the voltage waveforms can identify a short-circuit fault and facilitate the discrimination between faults that are either inside or outside of a set zone of the microgrid [21]. However, voltage-based protection may not be sensitive to high impedance faults (HIFs) and is therefore recommended as the backup protection.

Reference [22] proposes a traveling-wave based protection scheme. Here, the scheme adopts initial current traveling wavefronts as a main fault detection mechanism. However, the line length between different nodes of the microgrid is very short. Therefore, it is difficult to detect the initial wavefront.

A fault current source (FCS) can offer a large fault current in the case of a fault, and ensure the operation of the overcurrent relay [23]. However, the reliability and cost of the hardware limit the efficiency of this method.

The application of voltage information as a reference quantity for the detection of fault direction is a common practice in transmission lines. Nevertheless, this approach is not applicable in distribution networks due to the absence of potential transformers. Therefore, it is necessary to use the current-only polarity comparison for microgrids.

This paper presents a novel protection method for inverter-based microgrids using a current-only polarity comparison. The proposed method is based on the phase difference between the pre-fault current and the fault current components. The angle difference between the pre-fault current and the fault current components can be used to identify the faulted section. The proposed protection method can respond to faults in both grid-connected and autonomous operation modes.

The remainder of this paper is organized as follows. Section II provides an overview of the major protection issues in microgrids. Section III describes the proposed protection method for VSI-based microgrids. Section IV presents the simulation results for an inverter-based microgrid and protection system. Conclusions are drawn in Section V.

II. Fault Characteristics of Inverter-based Microgrids

Figure 1 shows the structure of the inverter-based microgrid considered in this paper. The microgrid model, modified from [24], is a medium-voltage microgrid consisting of inverter-based DERs. As shown in the figure, the microgrid is connected to the utility grid using a Δ/Y step-down transformer, and is a grounded system. In the microgrid, two feeders are connected to the point of common coupling (PCC) via a distribution line, and each feeder has a circuit breaker (CB) and current transformers (CTs). There are switchboards (SWBs) on each microgrid feeder, and CB1-CB3 are installed at each SWB. Two DERs are connected to the microgrid via a power electronic interface. A battery energy storage system (BESS) and a PV are connected to microgrid. Microgrids can operate in two modes: grid-connected and autonomous modes. In a grounded microgrid, there may be various paths for the ground return current in the case of a fault, because there are multiple grounded points in the distribution system. The CB installed at the end of the feeder and DER connection point can be used to isolate the fault area. The healthy section of the microgrid can be isolated from the fault section to eliminate the fault. The tie breaker between the two feeders can transfer the load to the healthy feeder if a fault occurs.

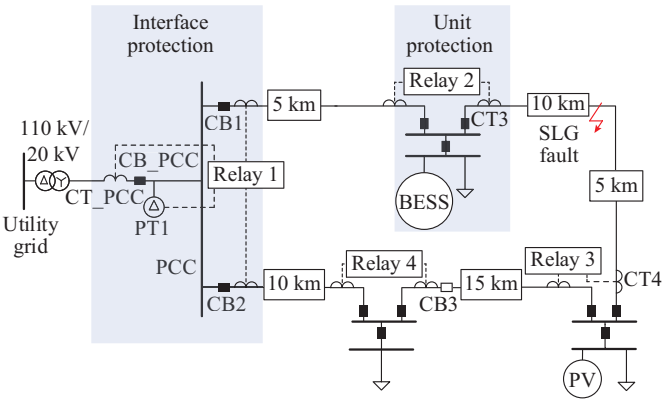

Fig. 1. Inverter-based medium voltage microgrid.

The protection system is a revised version of the one proposed in [25]. The method presented in [25] is adopted by using three zero-sequence current transformers to identify the faulted section. The method in this paper uses only two local measurement current signals.

The interface protection system can obtain the required information from the CTs at feeder 1, feeder 2, and the PCC bus. One potential transformer is installed on the PCC bus. The phase difference between pre-fault and fault current components is used for fault direction detection. The microgrid unit protection system shown in Fig. 1 collects the required information from the two CTs installed at SWB. The relay is situated locally and can detect the fault current and send polarity information to the microgrid control center. The interface protection at the PCC bus can identify the faulted feeder rapidly, and the unit protection system at SWB can identify the faulted section. The interface protection installed in the PCC bus will detect the voltage level as a backup for the protection system. Only when either the zero or negative sequence voltage increases or the three-phase voltage decreases, will the unit protection be unblocked. Then the unit protection system will identify the fault section.

The fault current levels of microgrids differ greatly between grid-connected and autonomous modes. The presence of DERs and complex operation scenarios of the microgrid can introduce challenges to protection. Additionally, the potentially large phase imbalance may make microgrid protection even more difficult. The investment in microgrid protection should also be considered. Moreover, inverter-based DERs can exhibit unconventional fault behaviors such as small short-circuit currents.

A simplified system network is shown in Fig. 2(a). In the figure, two sources are connected to buses *A* and *C*. The re-

lay is located in bus B and senses the current flow from bus B to bus C. We assume that the power flow direction is from bus A to bus C. The fault occurs at point F1. Z_{S1} and Z_{S2} are the source impedances; Z_{AB}, Z_{BF} and Z_{FC} are the line impedances; R_{BC} is the relay monitoring the current at bus B; and Δi_R is the fault current component. The proposed method uses the pre-fault current and fault current components for fault direction detection. The pre-fault current i_R can be given as:

$$i_R = \frac{|V_A|\angle 0°}{|Z_{AF1}|\angle\theta_1} = |I_{F1}|\angle(-\theta_1) \tag{1}$$

where $|V_A|\angle 0°$ is the pre-fault voltage at bus A; $|Z_{AF1}|\angle\theta_1$ is the line impedance between bus A and the fault point; I_{F1} is the pre-fault current magnitude; and θ_1 is the line impedance angle. The superimposed fault diagram of Fig. 2(a) can be shown as Fig. 2(b). The virtual voltage at bus B in the superimposed network is given by:

$$V_B = \Delta i_R (Z_{AB} + Z_{S1}) \tag{2}$$

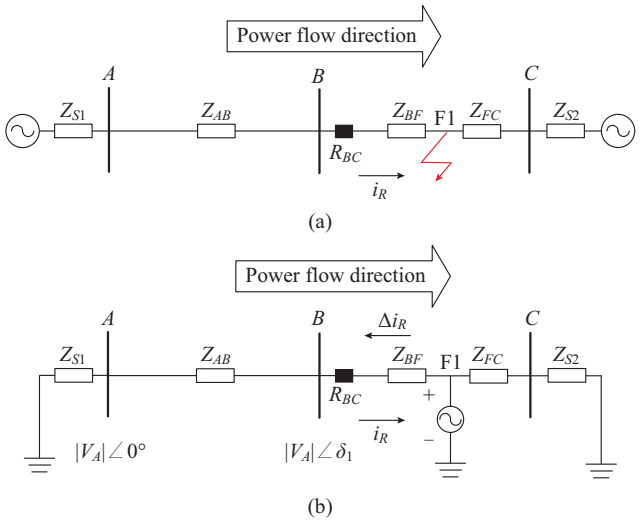

Fig. 2. Simplified diagram of pre-fault and superimposed fault systems (internal fault). (a) Pre-fault system. (b) Superimposed fault system.

The virtual voltage refers to the voltage variation. It is formed from the line impedance and fault current component. In the superimposed fault system, the voltage and current are in the opposite direction. Therefore, the polarity relationship between the current and virtual voltage is:

$$V_B i_R < 0 \tag{3}$$

Substituting (2) into (3) yields (4).

$$\Delta i_R (Z_{AB} + Z_{S1}) i_R < 0 \tag{4}$$

Formula (4) can be simplified to:

$$\Delta i_R i_R < 0 \tag{5}$$

From (5), when a fault occurs in the forward direction, the polarity between the pre-fault current and fault current components is reversed. Therefore, the fault direction can be identified. When the fault occurs at the backside of the measured point, the simplified system can be shown as in Fig. 3. Figure 3(a) shows the system diagram and Fig. 3(b) shows the superimposed diagram. The fault current components and pre-fault current polarities are studied herein.

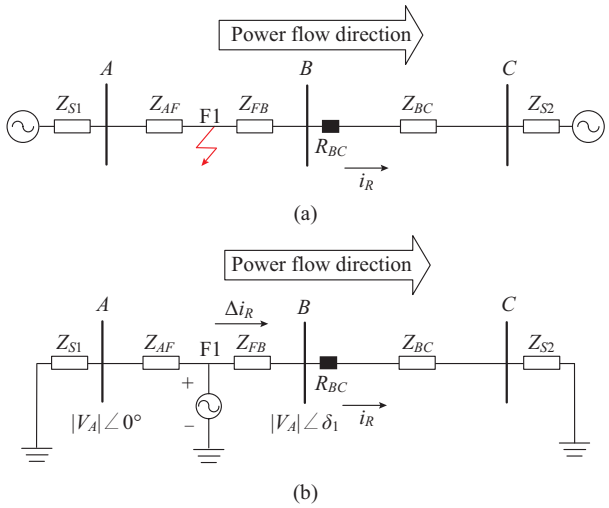

Fig. 3. Simplified diagram of pre-fault and superimposed fault systems (external fault). (a) Pre-fault system. (b) Superimposed fault system.

In the backward fault condition, the virtual voltage at bus B can be expressed by:

$$V_B = (Z_{BC} + Z_{S2})\Delta i_R \tag{6}$$

And the relationship between voltage and current is given by:

$$V_B i_R > 0 \tag{7}$$

Thus, the relationship between current and fault current components can be shown as:

$$\Delta i_R i_R > 0 \tag{8}$$

From (8), when a fault occurs in the backward direction, the polarity between the pre-fault current and fault current components is identical. The faulted section identification method is studied in Section III.

III. Proposed Protection Method

The phasor relationship between the pre-fault current and fault current components at the relay point is given by:

$$\cos\theta = \cos\left(\angle\left(I_R - \Delta i_R\right)\right) \tag{9}$$

The resulting $\cos\theta$ can be used as an indicator of the fault direction. The fault direction can be detected using the pre-fault current and the fault current components. When the fault occurs in the positive direction, $\cos\theta$ should be larger than zero, whereas when the fault occurs in the backward direction, $\cos\theta$ should be smaller than zero. Moreover, if the power flow direction is reversed, the polarity relationship between the pre-fault current and the fault component current is reversed. If $\cos\theta$ is larger than zero, the sign +1 is used to represent the forward fault. If $\cos\theta$ is smaller than zero, the sign –1 is used to represent the backward fault. The sign S is given as:

$$S = \begin{cases} 0 & \text{no event} \\ -1 & \cos\theta < 0 \\ +1 & \cos\theta > 0 \end{cases} \tag{10}$$

Before detecting the fault direction, it is necessary to detect the presence of a fault. As the short-circuit current is very small in the autonomous operation mode, a proper fault status detection method for autonomous microgrids is required. For this purpose, the fault condition should be checked. Equation (11) is based on the energy variation in fault current components.

$$\begin{cases} S_n = \int_{n-\pi/2}^{n} i_a(t)\mathrm{d}t \\ \Delta S = (S_n - S_{n-1}) - (S_{n-1} - S_{n-2}) \\ \Delta S \geq S_{Threshold} \end{cases} \tag{11}$$

where $i_a(t)$ denotes the current of phase A; S_n is the current energy in the n cycle; ΔS is the current energy variation; and $S_{Threshold}$ is the threshold value of current energy. The fault components can be calculated by:

$$\Delta i = i(k) - i(k - nN) \tag{12}$$

where N denotes the sampling number of each cycle. If the fault status and fault direction are detected, the fault section can be identified. The proposed unit protection system is based on local measurement of the current signal. The structure of the protection method is shown in Fig. 4. The unit protection system uses the pre-fault current as the fundamental basis for the detection of the fault direction, and the fault current component is used to identify the fault direction. The unit protection system compares the polarity between two adjacent CTs, and the polarity of local unit protection is sent to its adjacent unit protection through a communication channel. $\dot{I}_1$, $\dot{I}_2$, $\dot{I}_3$ and $\dot{I}_4$ represent the three-phase currents at CT1, CT2, CT3 and CT4, respectively.

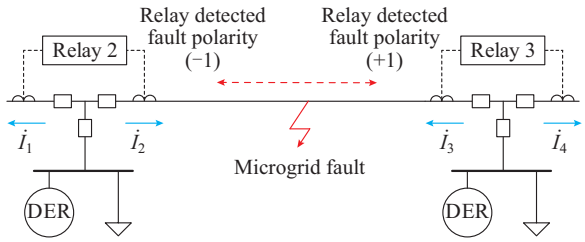

Fig. 4. Structure of proposed fault current based protection system.

Since the power flow direction in the microgrid changes over time, it is difficult to fix without voltage information. According to the analysis in Section II, the polarity detected by the relay at both ends of this section is reversed in the case of an internal fault. If a fault occurs externally, the polarity between the two adjacent CTs is the same. Hence, a new faulted section identification method is proposed. As shown in (13), the polarity of two adjacent CTs is multiplied, where −1 and +1 indicate the internal fault and external one, respectively.

$$S_i S_j = \begin{cases} 0 & \text{no event} \\ -1 & \text{internal fault} \\ +1 & \text{external fault} \end{cases} \tag{13}$$

To activate the unit protection system, a coordination strategy with a traditional protection system is applied, as shown in Fig. 5, where ΔI is the fault current components; D is the fault direction; and FS is the fault status. Three phase currents are used for the fault components calculator and the variation calculator. At the same time, the current is stored in the current storage block. The fault component and pre-fault current are compared to obtain the polarity of the fault direction, and the fault current energy variation is applied to determine the fault status. After the fault status and fault section are determined, the sign signal is compared with its adjacent sign signal. Finally, the CB trip signal is generated. Unit protection systems are equipped with a local intelligent electronic device (IED) to detect current variation according to a certain threshold. The IED then sends the gate signal to the protection system. After the fault status is determined, fault current based protection will identify the faulted section quickly. The faulted section can then be isolated, and other parts of the microgrid can be resupplied with power. A low-bandwidth communication system is required to achieve this, which can be realized through coordination with a traditional distribution protection system [26]-[28]. The detected sign of the adjacent CT is sent to the local CT and compared according to (13). If an internal fault occurs, CB at both ends will trip to isolate the faulted section. The only information transferred between different unit protection systems relates to polarity [29].

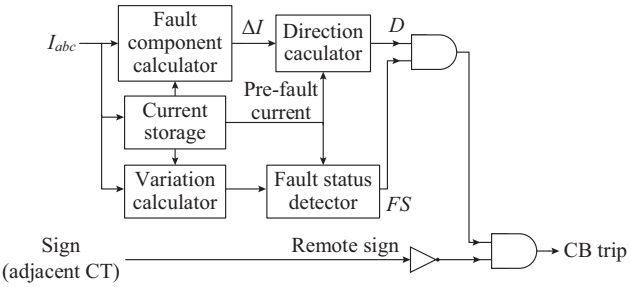

Fig. 5. Simplified schematic diagram of proposed unit protection method.

IV. Case Study

To determine the effectiveness of the proposed unit protection method, an inverter-based microgrid is simulated using PSCAD/EMTDC software, as shown in Fig. 6.

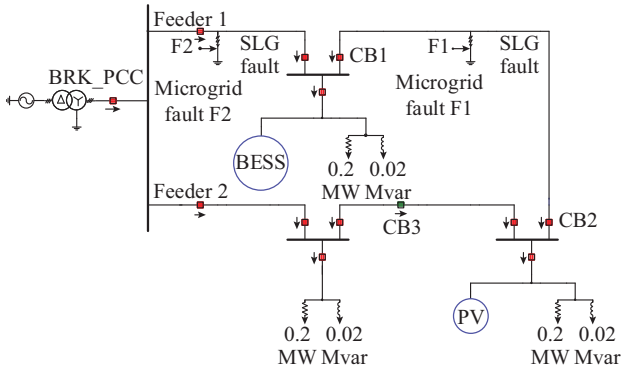

Fig. 6. PSCAD model of inverter-based microgrid.

The grid includes a 110 kV bus with a short-circuit capacity of 100 MVA. The distribution grid is grounded, and two

feeders are connected to the substation bus. Two DERs are connected at feeder 1 through an SWB, and one SWB supplies the load at feeder 2. There is a tie breaker, CB3, between feeders 1 and 2, which is normally open. In the case of a fault, CB3 is closed to supply power for the isolated section. And at the PCC, there is a breaker BRK_PCC. There is a single line-to-ground (SLG) fault at feeder 1. Moreover, there are measurement points on either side of the fault.

The parameters of the microgrid are shown in Table I. In the microgrid, a BESS is used to maintain the voltage and current in autonomous mode. The battery can supply power for an islanded area. The BESS allows storage and discharge of the electric power to achieve economic advantage. The BESS in the microgrid is controlled using the constant voltage and constant frequency (CVCF) method. The different control mode may change the fault-current angle. However, the method proposed in this paper is not affected by the different control modes because it is based on the phase difference between pre-fault current and fault-current components [30]-[34].

TABLE I
SYSTEM CONFIGURATION

System component	Parameter
Step-down transformer (△/Y)	110 kV/20 kV
System frequency	50 Hz
BESS capacity	0.40 MW
PV capacity	0.40 MW
Fault resistance	0.01 Ω

The simulation results of the microgrid are shown in Fig. 7, where RMS represents root-mean-square. The microgrid changes from grid-connected mode to autonomous mode in 1.0 s, and the voltage and frequency decrease initially. Then the DER initiates the control of voltage and frequency, which stabilizes after 1.5 s.

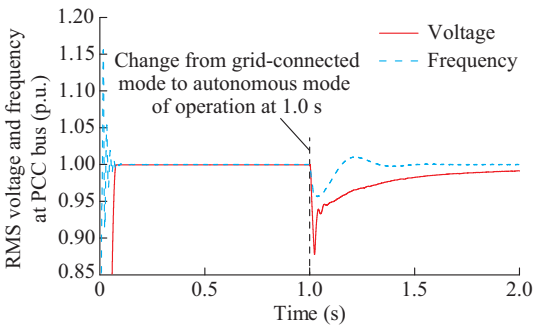

Fig. 7. Simulation results of inverter-based microgrid.

The voltage and current signals are pre-conditioned using a second-order Butterworth low-pass filter to prevent anti-aliasing errors, and a discrete Fourier transform (DFT) has been used to estimate the sequence components. The SLG fault is initiated in autonomous operation mode at feeder 1. Figure 8 shows the three-phase current of CT3. The output current of DER is limited and the fault current is not large enough for conventional overcurrent relay.

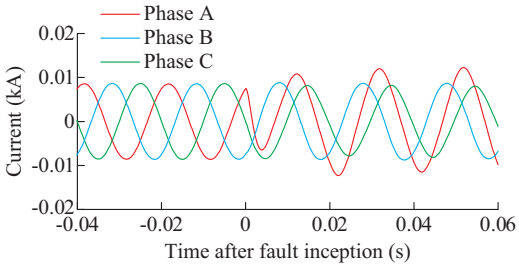

Fig. 8. Three-phase currents after fault inception.

The variation in current energy during a fault is shown in Fig. 9. The magnitude of the variations increases during the fault period. This can be exploited to facilitate the fault status detection. And the physics essence of current energy is the quantity of electric charge. If the current energy variation exceeds a threshold value, the relay will detect the fault.

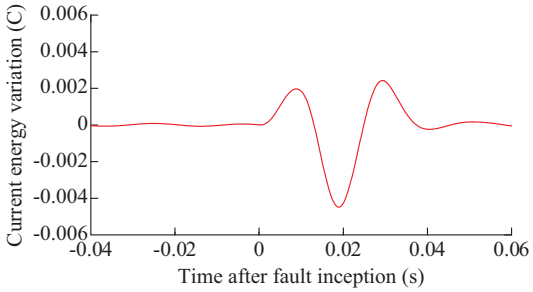

Fig. 9. Fault current energy variation of phase A during a fault.

The fault current components during a fault are shown in Fig. 10. To detect all types of faults, the positive-sequence current is used since it exists in both normal and fault conditions. As shown in the figure, the positive-sequence current angle difference between the fault current components and the pre-fault current can be used to generate the sign of the fault direction. In Fig. 10(a), the positive-sequence current decreases after a fault. In Fig. 10(b), the positive-sequence current increases after a fault. Moreover, the fault current component is the difference between the normal positive-sequence current and the fault positive-sequence one. In the simulation, two fault current component cycles are generated. The phasor information of the fault current components is used for determining the fault direction, while the pre-fault positive-sequence current is the base of the fault direction. In addition, the fault direction is related to the power flow direction; thus, (13) can be used for fault section identification. After two cycles of delay shift of the pre-fault current, the polarity between the pre-fault and fault current components is clear.

As shown in Fig. 11, for the pre-fault current and fault current components, the polarity is reversed in CT3 and remains the same in CT4. Therefore, there is a fault between CT3 and CT4.

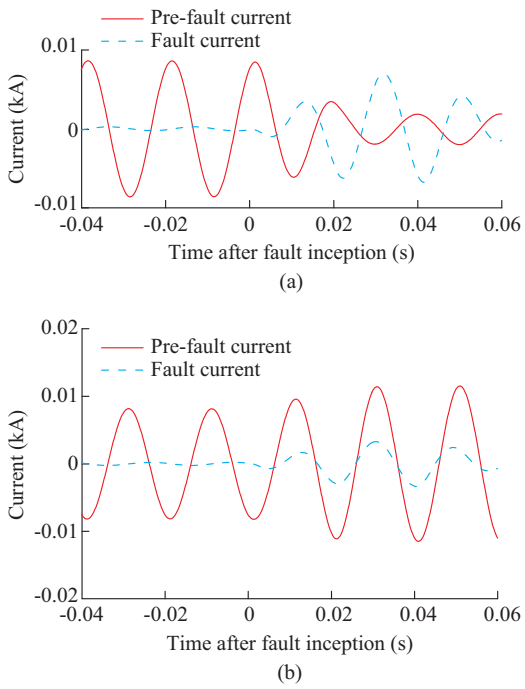

Fig. 10. Positive-sequence pre-fault and fault current components in CT3 and CT4. (a) Current in CT3. (b) Current in CT4.

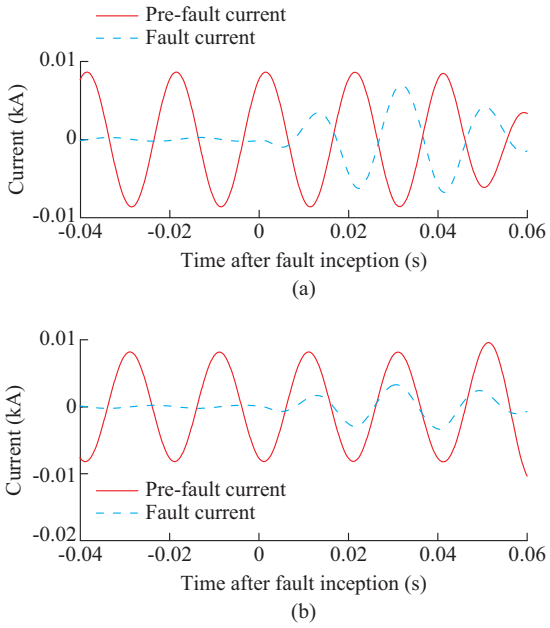

Fig. 11. Positive-sequence pre-fault and fault current components in CT3 and CT4. (a) Two cycles delay in CT3. (b) Two cycles delay in CT4.

To compare the polarity between pre-fault current and fault current components, a phase difference calculation is done using the DFT algorithm, and the sign values are determined based on (10). Figure 12 shows the calculation results for cos θ. In the case of the SLG fault in position F1, CT3 detects the sign value of −1 and CT4 detects the sign value of +1. The opposite signs indicate that there is an internal fault between CT3 and CT4.

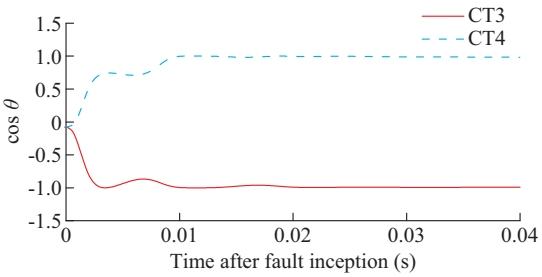

Fig. 12. Phase difference calculation results.

To determine the validity of the algorithms, an external fault is also tested. If a fault occurs at position F2, the measurement currents shown in Fig. 13 for CT3 and CT4 occur. As shown in the figure, if there is an external fault, the polarity of the pre-fault current and fault current components is identical. According to (13), there is an external fault.

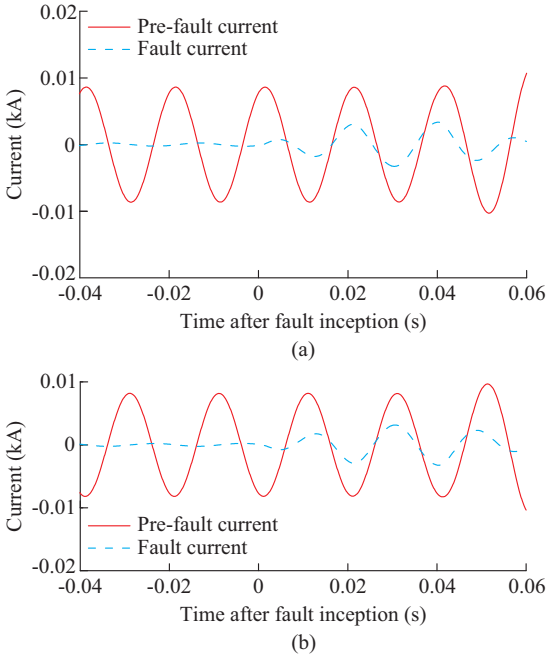

Fig. 13. Positive-sequence pre-fault and fault current components in CT3 and CT4 (external fault). (a) Two cycles delay in CT3. (b) Two cycles delay in CT4.

Table II shows the result in different fault conditions. In the table, G stands for the grid-connected mode; A stands for the autonomous mode; and R stands for the fault resistance. We can see that the proposed method works in both grid-connected and autonomous modes. Different fault resistances are tested and it is demonstrated that the proposed method can respond to faults with different resistances. Also, for different fault types, the proposed method can work well. The simulation results show that this method can protect the microgrid against faults with different fault resistances and different types. And the proposed method is not affected by the microgrid operation condition. In any case, the proposed method can protect microgrid and identify the internal fault section effectively.

TABLE II
TEST RESULTS

Fault type	Result of G			Result of A		
	$R=0.1\,\Omega$	$R=10\,\Omega$	$R=100\,\Omega$	$R=0.1\,\Omega$	$R=10\,\Omega$	$R=100\,\Omega$
Single-line-to-ground (SLG)	–1	–1	–1	–1	–1	–1
Double-line-to-ground (LLG)	–1	–1	–1	–1	–1	–1
Line-to-line (LL)	–1	–1	–1	–1	–1	–1
Three-phase-to-ground (LLLG)	–1	–1	–1	–1	–1	–1
Three-phase (LLL)	–1	–1	–1	–1	–1	–1

V. CONCLUSION

In this paper, a novel protection method for inverter-based microgrid using current-only polarity comparison is proposed. The method uses the phase difference between the pre-fault current and fault current components to detect the fault direction. Using the proposed method, the internal faulted section can be identified in an autonomous microgrid. The inverter-based microgrid model is simulated using PSCAD/EMTDC software, and the signal is processed using MATLAB. The results show that the proposed method can detect faults in inverter-based microgrids.

REFERENCES

[1] N. Hatziargyriou, H. Asano, R. Iravani *et al*., "Microgrids," *IEEE Power & Energy Magazine*, vol. 5, no. 4, pp. 78-94, Jul.-Aug. 2007.

[2] R. H. Lasseter, "Smart distribution: coupled microgrids," *Proceedings of the IEEE*, vol. 99, no. 6, pp. 1074-1082, Jun. 2011.

[3] M. A. Zamani, T. S. Sidhu, and A. Yazdani, "A protection strategy and microprocessor-based relay for low-voltage microgrids," *IEEE Transactions on Power Delivery*, vol. 26, no. 3, pp. 1873-1883, Jul. 2011.

[4] K. O. Oureilidis and C. S. Demoulias, "A fault clearing method in converter-dominated microgrids with conventional protection means," *IEEE Transactions on Power Electronics*, vol. 31 no. 6, pp. 4628-4640, Jun. 2016.

[5] M. A. Zamani, A. Yazdani, and T. S. Sidhu, "A control strategy for enhanced operation of inverter-based microgrids under transient disturbances and network faults," *IEEE Transactions on Power Delivery*, vol. 27, no. 4, pp. 1737-1747, Oct. 2012.

[6] M. A. Zamani, A. Yazdani, and T. S. Sidhu, "A communication-assisted protection strategy for inverter-based medium-voltage microgrids," *IEEE Transactions on Smart Grid*, vol. 3, no. 4, pp. 2088-2099, Dec. 2012.

[7] H. Al-Nasseri, M. A. Redfern, and F. Li, "A voltage based protection for micro-grids containing power electronic converters," in *Proceedings of IEEE PES General Meeting*, Montreal, Canada, Jun. 2006, pp. 1-7.

[8] R. Majumder, M. Dewadasa, A. Ghosh *et al*., "Control and protection of a microgrid connected to the utility through back-to-back converters," *Electric Power Systems Research*, vol. 81, no. 7, pp. 1424-1435, Jul. 2011.

[9] E. Sortomme, J. Ren, and S. S. Venkata, "A differential zone protection scheme for microgrids," in *Proceedings of IEEE PES General Meeting*, Vancouver, Canada, Jul. 2013, pp. 1-5.

[10] H. Laaksonen, D. Ishchenko, and A. Oudalov, "Adaptive protection and microgrid control design for Hailuoto Island," *IEEE Transactions on Smart Grid*, vol. 5, no. 3, pp. 1486-1493, May 2014.

[11] S. A. Gopalan, V. Sreeram, and H. H. C. Iu, "A review of coordination strategies and protection schemes for microgrids," *Renewable and Sustainable Energy Reviews*, vol. 32, pp. 222-228, Apr. 2014.

[12] S. Mirsaeidi, D. M. Said, M. W. Mustafa *et al*., "Progress and problems in micro-grid protection schemes," *Renewable and Sustainable Energy Reviews*, vol. 37, pp. 834-839, Sept. 2014.

[13] S. Mirsaeidi, X. Dong, S. Shi *et al.*, "Challenges, advances and future directions in protection of hybrid AC/DC microgrids," *IET Renewable Power Generation*, vol. 11, no. 12, pp. 1495-1502, Oct. 2017.

[14] W. K. A. Najy, H. H. Zeineldin, and L. W. Wei, "Optimal protection coordination for microgrids with grid-connected and islanded capability," *IEEE Transactions on Industrial Electronics*, vol. 60, no. 4, pp. 1668-1677, Apr. 2013.

[15] H. Yazdanpanahi, W. Xu, and Y. W. Li, "A novel fault current control scheme to reduce synchronous DG's impact on protection coordination," *IEEE Transactions on Power Delivery*, vol. 29, no. 2, pp. 542-551, Apr. 2014.

[16] N. Rajaei, M. H. Ahmed, M. M. A. Salama *et al*., "Fault current management using inverter-based distributed generators in smart grids," *IEEE Transactions on Smart Grid*, vol. 5, no. 5, pp. 2183-2193, Sept. 2014.

[17] D. M. Bui, S. L. Chen, K. Y. Lien *et al.*, "Fault protection solutions appropriately used for ungrounded low-voltage AC microgrids," in *Proceedings of Innovative Smart Grid Technologies – Asia*, Bangkok, Thailand, Nov. 2015, pp. 1-6.

[18] A. K. Sahoo, "Protection of microgrid through coordinated directional over-current relays," in *Proceedings of Global Humanitarian Technology Conference – South Asia Satellite*, Trivandrum, India, Sept. 2014, pp. 129-134.

[19] M. Dewadasa, A. Ghosh, and G. F. Ledwich, "Distance protection solution for a converter controlled microgrid," in *Proceedings of the 15th National Power Systems Conference (NPSC)*, Bombay, India, Dec. 2008, pp. 586-591.

[20] E. Casagrande, W. L. Woon, and H. H. Zeineldin, "A differential sequence component protection scheme for microgrids with inverter-based distributed generators," *IEEE Transactions on Smart Grid*, vol. 5, no. 1, pp. 29-37, Jan. 2014.

[21] H. Al-Nasseri, M. A. Redfern, and R. O'Gorman, "Protecting microgrid systems containing solid-state converter generation," in *Proceedings of International Conference on Future Power Systems*, Amsterdam, Netherlands, Nov. 2005, pp. 1-5.

[22] X. Li, A. Dyśko, and G. M. Burt, "Traveling wave-based protection scheme for inverter-dominated microgrid using mathematical morphology," *IEEE Transactions on Smart Grid*, vol. 5, no. 5, pp. 2211-2218, Sept. 2014.

[23] F. V. Overbeeke, "Fault current source to ensure the fault level in inverter-dominated networks," in *Proceedings of International Conference and Exhibition on Electricity Distribution*, Prague, Czech Republic, Jun. 2009, pp. 1-4.

[24] H. Laaksonen, "Protection scheme for island operated medium-voltage microgrid," *International Review of Electrical Engineering*, vol. 10, no. 4, pp. 510-519, Aug. 2015.

[25] L. Jing, D. H. Son, S. H. Kang *et al.*, "A novel protection method for single line-to-ground faults in ungrounded low-inertia microgrids," *Energies*, vol. 9, no. 6, pp. 1-16, Jun. 2016.

[26] X. Dong, D. Wang, M. Zhao *et al.*, "Smart power substation development in China," *CSEE Journal of Power & Energy Systems*, vol. 2, no. 4, pp. 1-5, Dec. 2016.

[27] J. He, L. Liu, F. Ding *et al*., "A new coordinated backup protection scheme for distribution network containing distributed generation," *Protection & Control of Modern Power Systems*, vol. 2, no. 1, pp. 1-10, Dec. 2017.

[28] Y. H. Wu, X. Z. Dong, and S. Mirsaeidi, "Modeling and simulation of air-gapped current transformer based on Preisach theory," *Protection & Control of Modern Power Systems*, vol. 2, no. 1, pp. 1-11, Dec. 2017.

[29] K. Lai, M. S. Illindala, and M. A. Haj-Ahmed, "Comprehensive protection strategy for an islanded microgrid using intelligent relays," *IEEE Transactions on Industry Applications*, vol. 53, no. 1, pp. 47-55, Jan.-Feb. 2017.

[30] L. Qiao, X. Li, D. Huang *et al*., "Coordinated control for medium voltage DC distribution centers with flexibly interlinked multiple microgrids," *Journal of Modern Power Systems and Clean Energy*, vol.

7, no. 3, pp. 599-611, May 2019.
[31] Y. Du, W. Pei, N. Chen *et al*., "Real-time microgrid economic dispatch based on model predictive control strategy," *Journal of Modern Power Systems and Clean Energy*, vol. 5. no. 5, pp. 787-796, Sept. 2017.
[32] B. Liu, "System deployment and decentralized control of islanded AC microgrids without communication facility," *Journal of Modern Power Systems and Clean Energy*, vol. 7, no. 4, pp. 913-922, Jul. 2019.
[33] L. Zhu, X. Zhou, X. Zhang *et al*., "Integrated resources planning in microgrids considering interruptible loads and shiftable loads," *Journal of Modern Power Systems and Clean Energy*, vol. 6, no. 3, pp. 1-14, May 2018.
[34] L. Che, X. Shen, and M. Shahidehpour, "Primary frequency response based rescheduling for enhancing microgrid resilience," *Journal of Modern Power Systems and Clean Energy*, vol. 7, no. 4, pp. 696-704, Jul. 2019.

Bin WANG received the B.Sc. degree in electrical engineering from Shandong University of Technology, Zibo, China, in 1999, and Ph.D degree from Shandong University, Jinan, China in 2005. From July 2005 to December 2010, he has been working as a post doctoral fellow and assistant researcher at Tsinghua University, Beijing, China. He now serves as an Associate Professor at Tsinghua University. From December, 2013, he works as a visiting scholar in CURENT center, University of Tennessee, Knoxville, USA. His main research interests are power system protection, substation automation based on IEC 61850 and power quality.

Liuming JING received the B.Sc. degree in electrical engineering from Hunan University, Changsha, China, in 2011, and the Ph.D. degree in electrical engineering from Myongji University, Yongin, Korea, in 2017. Currently, he is working as a postdoctoral fellow at Tsinghua University, Beijing, China. His research interests are power system control and protection.